SENSITIVITY STUDY OF AN OPAQUE VENTILATED FAÇADE IN THE WINTER SEASON IN DIFFERENT CLIMATE ZONES IN SPAIN

F. Peci López, M. Ruiz de Adana Santiago.

*Departamento de Química-Física y Termodinámica Aplicada – Escuela Politécnica Superior. Universidad de Córdoba,
Campus de Rabanales. Antigua Carretera Nacional IV, km 396.
14014 Córdoba – España
qf1pelof@uco.es
tlf/fax: +034957212236

Abstract: Energy efficient buildings need to take advantage of any renewable energy available. An opaque ventilated façade (OVF) is a kind of façade that absorbs solar energy and transfers it to the ventilation system. This way, the sensible ventilation load of the heating system can be reduced in the winter season. The energy saving of this system depends strongly on the weather variables, mainly solar radiation on the façade, ambient temperature and wind speed. In order to find the most convenient locations where the best OVF efficiency can be obtained, its performance has to be studied along a complete season. For this purpose in this study a sensitivity analysis with the most important weather variables was carried out and the energy saving values in 12 locations in Spain in the winter were evaluated using a numerical model previously validated with experimental data. The results showed that although the most influential weather variable was solar radiation, a combination of high temperatures and low wind speeds can also lead to important energy saving values. It was found that the most convenient locations for installing an OVF were those with low and medium winter severity climates, namely, in the southern and coastal regions of Spain (zones A3, B3, B4, C3 and C4).

Keywords: Natural ventilation. Opaque ventilated façade. Ventilated façade. Energy Saving. Sensitivity study. Energy efficient building.

1. Introduction

The energy consumption of buildings accounts for approximately 40% of the total amount of energy used in a country. This energy is mainly used in the heating, ventilation and air conditioning systems. Thus, installing devices based on the renewable sources of energy available for buildings is an interesting alternative to reduce the consumption of electricity and conventional fuels, and therefore to lower emissions of greenhouse effect gases.

Solar energy has been used traditionally throughout solar collectors, converting the solar radiation absorbed in thermal energy using a storage fluid or in electricity using photovoltaic panels. Solar energy is also usually transferred to the inner spaces directly through the building windows and through the façade walls by conduction heat transfer. However façades walls are traditionally designed to insulate the inner space from the environment in the winter so the solar radiation that is absorbed by the external surface of the façade is normally transferred to the ambient air by convection and long wave radiation interchange. The traditional way of using the solar energy to heat indoor spaces in the winter is by letting the solar radiation go in through transparent layers, mainly windows or glazed panels. However, high glazed façades have a high risk of overheating in the summer season, mainly in hot and dry climates.

One way to prevent overheating that has been widely studied in literature is the use of transparent double skin façades [1]. This kind of façades are generally made up of two glazed layers with an air gap in between. A shading system is placed in the air gap to absorb the solar radiation and transfer the heat to the air inside the façade. This air can be exhausted in case of overheating or introduced into the building to provide preheated ventilation air to the inner spaces. However the use of highly glazed buildings implies higher costs of materials, construction and maintenance, and still the risk of overheating in hot climates [2, 3].

An opaque ventilated façade (OVF) is an interesting, simple and economical alternative for using the solar radiation in a building. In this kind of double skin façade both solid layers are opaque. The external one is used to absorb the solar energy and to transfer part of it to the air in the gap. The inner layer acts as the insulation layer. This way the risk of overheating in the summer is avoided and yet part of the solar energy can be used to heat the ventilation air in the winter season.

Many types of OVF's have been studied so far, and a review of them can be checked in [4]. In some cases the OVF is combined with other energy systems [5-7]. Some OVF are called open joint ventilated façades [8, 9], they consist in rows or tiles separated from each other a certain distance. The benefits of using this kind of façade can be read in [10, 11]. The most popular OVF's are those in which its external layer is made of ceramic, clay or stone [12, 13], but it could be also made of metal [14].

Another way of using the solar energy received by the building is the use of the so called unglazed transpired collector (UTC). This kind of solar collector appeared at the early nineties and have been installed in a number of buildings, [15-18]. OVF's and UTC's are both opaque solar absorbers. An UTC reduces the external convection heat loss by suction of the external heat boundary layer [19]. A comparison between an OVF and an UTC was carried out in [20] showing that UTC's have better efficiency than OVF's. Nevertheless, an OVF is a simpler system, and when there is no need for high ventilation rates and materials and installation costs are critical, it can reduce the heating energy consumption considerably. Furthermore, an OVF can be a versatile system, as it can adopt several modes of operation depending on the aperture of its openings [21]. This modes of operation can work with mechanical or natural ventilation[22], which can be buoyancy or wind driven [23].

The annual energy saving that can be obtained by an OVF strongly depends on the location of the building and thus on its climate conditions. Therefore, it would be interesting to know which weather variables most influence the energy saving in order to establish which locations are more favourable for installing an OVF system.

The objective of this paper is to find the weather characteristics of the better locations for installing an OVF system and which weather variables influence the most on the reduction of the sensible heat demand of the building. To do this, a sensibility analysis was done to detect the most influential weather variable and simulations were carried out for a building with and without an OVF in the different climate zones in Spain.

2. Methodology

Numerical Model

An experimentally validated numerical model of OVF was used to carry out the simulations of the building energy performance. The details of this model were explained in [24]. This model was included in the building model created using the building energy simulation software TRNSYS [25].

Case study

The selected building was a typical four storey box shaped office building, figure 1. The room studied was an office room of 8 x 7 x 3.25 m, see figure 2. The room had four OVF modules of 1 m width each, covering half of the surface of the south façade. The conventional part of the south façade had windows covering half its area. The entire north façade was conventional. The rest of walls, the floor and the ceiling limited with other similar office rooms. The materials used in each wall and their properties can be seen in tables 1, 2 and 3.

The room was provided with mechanical ventilation which entered the inner space through the OVF. The air gap of each module of OVF can be considered a 1 m width and 0.05 m depth duct. The air entered the OVF through the lower opening of the external layer and was introduced in the room through the upper opening in the insulation layer, see figure 3. The latter opening was opened or closed using a trap door. The air was exhausted from the room through a ventilation duct in the room ceiling, which went up to the roof of the building. This duct had a square cross section of 0.50 m width and roughness 0.1 mm. It had a grill with dynamic loss coefficient of 2.161.

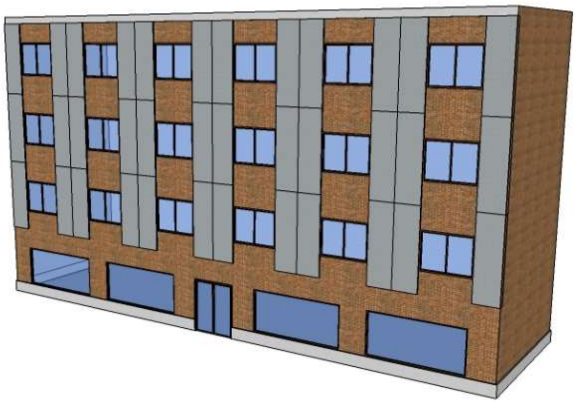

Figure 1. Building sketch.

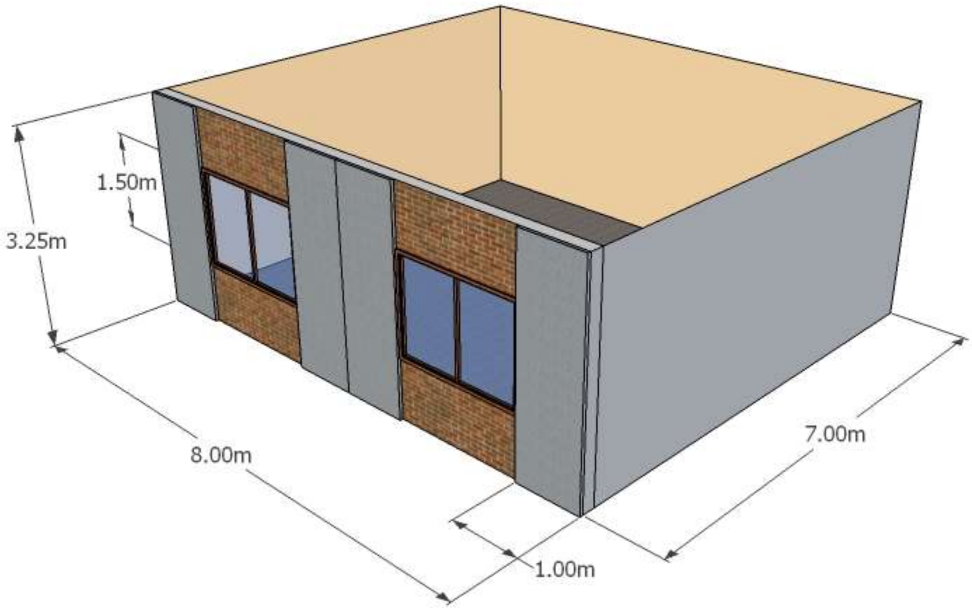

Figure 2. Dimensions of the room studied

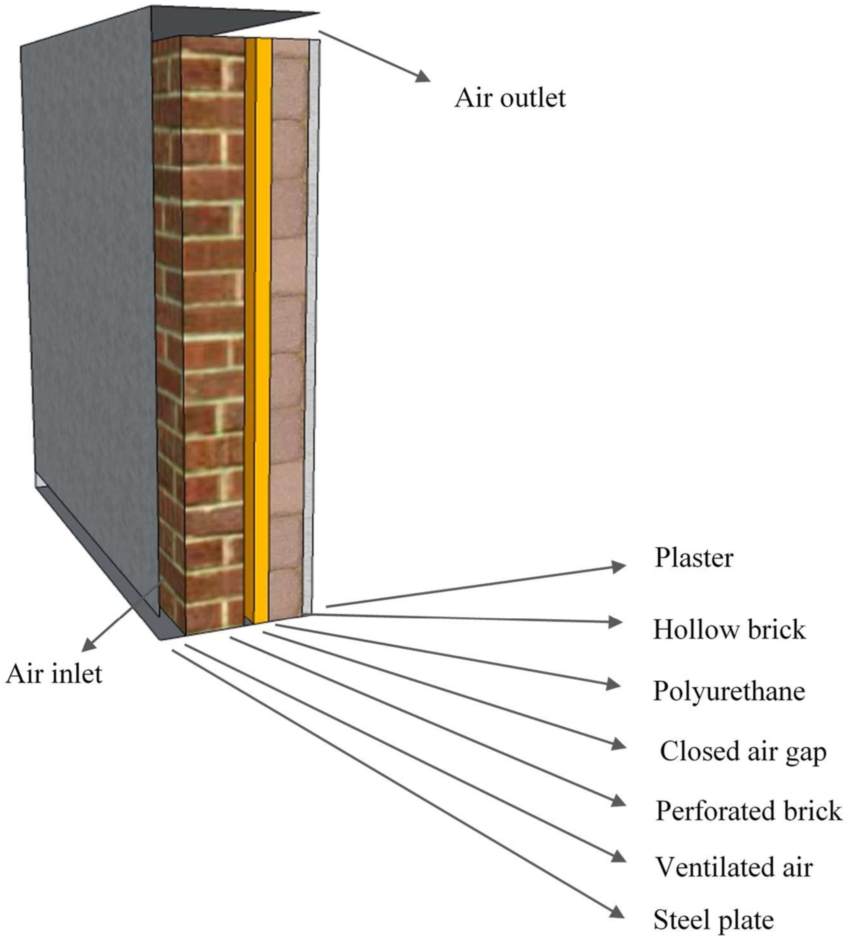

Figure 3. Façade layers including OVF

Table 1. Thermophysical properties of wall materials

Layer	Material	Thickness (m)	Density (kg/m^3)	Specific Heat (kJ/kg K)	Conductivity (W/m K)	Thermal Resistance (m^2 K /W)
1	Plaster	0.020	900	1	0.26	0.077
2	Hollow brick	0.070	1200	0.9	0.42	0.166
3	polyurethane	0.030	30	1.5	0.02	1.500
4	Air	0.020	1	1	0.02	1.000
5	Perforated brick	0.115	1600	1	0.65	0.177
6 *	Air	0.050	1	1	0.02	1.000
7 *	Galvanized Steel	0.001	-	-	-	$5.54x10^{-5}$

*Only in the case with OVF

Table 2. Properties of window panes

Glazing	Thickness (m)	u-value (W/m^2K)	g-value	Area (m^2)
Single pane	0.006	5.73	0.837	6.50

Table 3. Radiative properties of façade surfaces

Surfaces	Area (m^2)	Absorptivity	Material
Brick	6.50	0.36	Dark Brown brick
Steel plate	13.0	0.70	Light grey galvanized Steel

The working time schedule was established from 9:00 am to 5:00 pm from Monday to Friday. It was established a number of 6 people in the room with a degree of activity 4 according to [26] (Seated, light work, typing). Each person used an 80 W computer terminal. The illumination consisted of fluorescent lamps with a power rate of 10 W/m^2. The light was set always on during the working time. The room air temperature was set to 21 ºC and the relative humidity to 50 % in the working time. The energy transferred to the space air to maintain these conditions were calculated in the simulations.

The ventilation airflow rate was established according to the Spanish regulation [27], corresponding to very good indoor air quality, IDA 2. According to this, 12.5 m^3 of air per person was needed. A density of occupation of 9 m^2/person was considered which made a total of 6 people and thus a ventilation air flow rate of 270 m^3/h.

The wind pressure on the external surface of the building was taken into account through the pressure coefficient C_p, which is defined with equation (1).

$$P_w = C_P \frac{\rho V^2}{2} \quad (1)$$

Where P_w is the difference between static pressure on the façade and atmospheric pressure (Pa), ρ is the air density (kg/m^3) and V is the wind speed (m/s), which is normally taken at the roof level. The pressure coefficients were calculated using the CpCalc+ software package [28], and they can be seen in table 4.

Table 4. Pressure coefficients

	Pressure Coefficients (C_P)							
Angle of incidence	**0**	**45**	**90**	**135**	**180**	**225**	**270**	**315**
Ground floor north	0.0668	0.0220	-0.0451	-0.0216	-0.0205	-0.0216	-0.0451	0.0220
Ground floor East	-0.0984	0.0191	0.0587	0.0191	-0.0984	-0.0471	-0.0445	-0.0471
Ground floor south	-0.0205	-0.0216	-0.0451	0.0220	0.0668	0.0220	-0.0451	-0.0216

Ground floor west	-0.0984	-0.0471	-0.0445	-0.0471	-0.0984	0.0191	0.0587	0.0191
1st floor north	0.0365	0.0120	-0.0565	-0.0273	-0.0258	-0.0273	-0.0565	0.0120
1st floor east	-0.1180	0.0126	0.0383	0.0126	-0.1180	-0.0566	-0.0535	-0.0566
1st floor south	-0.0258	-0.0273	-0.0565	0.0120	0.0365	0.0120	-0.0565	-0.0273
1st floor west	-0.1180	-0.1180	-0.0535	-0.0566	-0.1180	0.0126	0.0383	0.0126
2nd floor north	0.1602	0.0518	-0.0529	-0.0249	-0.0248	-0.0249	-0.0529	0.0518
2nd floor east	-0.1134	0.0601	0.1860	0.0601	-0.1134	-0.0531	-0.0527	-0.0531
2nd floor south	-0.0248	-0.0249	-0.0529	0.0518	0.1602	0.0518	-0.0529	-0.0249
2nd floor west	-0.1134	-0.0531	-0.0527	-0.0531	-0.1134	0.0601	0.1860	0.0601
3rd floor north	0.4205	0.1321	-0.0623	-0.0278	-0.0293	-0.0278	-0.0623	0.1321
3rd floor east	-0.1479	0.1228	0.3905	0.1228	-0.1479	-0.0661	-0.0694	-0.0661
3rd floor south	-0.0293	-0.0278	-0.0623	0.1321	0.4205	0.1321	-0.0623	-0.0278
3rd floor west	-0.1479	-0.0661	-0.0694	-0.0661	-0.1479	0.1228	0.3905	0.1228
Roof	-0.0150	-.0160	-.0.0210	-0.0160	-0.0150	-0.0160	-0.0210	-0.0160

The external convection heat transfer coefficients were calculated according to [29] using the expressions (2) and (3).

$$H_{ext}=4.8+1.7\ V_f\ (\text{windward}) \qquad (2)$$

$$H_{ext}=2.6+2.5\ V_f\ (\text{leeward}) \qquad (3)$$

Where V_f is the wind speed at the height of the roof.

Control strategy

The inner trap door was kept always open during working time while the mechanical ventilation provided the room with the required air flow rate. During the non-working period the trap door opened following a hysteresis cycle that had a lower temperature of 21 ˚C and an upper temperature of 23 ˚C. Whenever the temperature was over the upper temperature limit the trap opened to provide the room with ventilation at a convenient temperature, whereas the trap was closed when the air temperature went down below the lower limit. Thus instability was avoided in the performance of the trap door. The OVF efficiency was evaluated using the expression [20]:

$$\eta_{coll} = \frac{\dot{m}\ c_p(T_{out}-T_{amb})}{I_s A} \qquad (4)$$

Where $\dot{m}$ is the mass flow rate (kg/s), c_p is the air specific heat (J/kg ˚C), T_{out} is the OVF outlet air temperature, T_{amb} is the ambient temperature, I_s is the intensity of solar radiation on the external surface (W/m^2), and A is the external surface area (m^2).

The same building but without OVF modules was used for comparison purposes. In this building the ventilation was taken directly from outdoor. The same ventilation strategy as the first building was followed and the openings had the same dimensions as all the OVF trap doors in the first case. Thus, both buildings were comparable regarding the use of outdoor air for ventilation.

Simulations

In order to determine the influence of temperature, solar radiation and wind speed on the heating energy saving a two-way ANOVA analysis was carried out. This kind of analysis gives information about the influence of the variables considered and its interactions on the system output [30]. For this purpose a matrix of cases with three variables with five levels each was built, yielding a number of 125 cases. The levels were selected equally spaced between the minimum and maximum day evolution of the variable found in the weather data files used for this study. Both buildings, with and without OVF were simulated in each case. In figure 4 the levels of temperature, solar radiation and wind speed can be seen. The simulation period was one day and the time step was 1 h.

For the second set of simulations twelve locations were considered to analyse the influence of climatic conditions on the energy saving obtained using an OVF system during the winter season. These locations were selected according to table 6 which classifies locations depending on their winter and summer severity in Spain [31], as this country has enough climate variability for the current study, figure 5. Mediterranean, continental and oceanic climates can be found in Spain.

The correspondence between the climatic zone code and the climate severity indexes is shown in table 5, where the winter and summer severity indexes are calculated using the following expressions[31]:

$$SCI = -8.35 \cdot 10^{-3} Rad + 3.72 \cdot 10^{-3} GD - 8.62 \cdot 10^{-6} + \quad (5)$$

$$+4.88 \cdot 10^{-5} (Rad)^2 + 7.15 \cdot 10^{-2} (GD)^2 - 6.81 \cdot 10^{-2}$$

or the alternative formula:

$$SCI = 2.395 \cdot 10^{-3} GD - 1.111 \left({}^{n}/_{N} \right)^2 + 1.885 \cdot 10^{-6} (GD)^2 + \quad (6)$$

$$+7.026 \cdot 10^{-1} ({}^{n}/_{N})^2 + 5.709 \cdot 10^{-2}$$

For the summer:

$$SCV = 3.724 \cdot 10^{-3}\, Rad + 1.409 \cdot 10^{-2}\, GD - 1.869 \cdot 10^{-5} Rad\, GD - \quad (7)$$

$$-2.053 \cdot 10^{-6} (Rad)^2 - 1.389 \cdot 10^{-5} (GD)^2 - 5.434 \cdot 10^{-1}$$

or the alternative formula:

$$SCV = 1.090 \cdot 10^{-2} GD + 1.023 \left({}^{n}/_{N} \right) - \quad (8)$$

$$-1.638 \cdot 10^{-5} (GD)^2 - 5.977 \cdot 10^{-1} ({}^{n}/_{N})^2 - 3.370 \cdot 10^{-1}$$

Where GD is the mean degree days in winter with base 20 for January, February and December, Rad is the mean accumulated global radiation for January, February and December (kW h/m2) and n/N is the ratio of sun hours to maximum sun hours summed up separately for January, February and December.

Table 5. Summer and winter severity codes.

Winter Climate Severity				
A	B	C	D	E
SCI≤0.3	0.3<SCI≤0.6	0.6<SCI≤0.95	0.95<SCI≤1.3	SCI>1.3
Summer Climate Severity				
1	2	3	4	5
SCV≤0.6	0.6<SCV≤0.9	0.9<SCV≤1.25	0.9<SCV≤1.25	SCV>1.25

Despite the selection of these locations, in this piece of work the influence of the weather variables on the energy saving was found, and thus a broader study can be done afterwards to obtain the best locations in other countries or regions. The weather files corresponded to typical meteorological year data extracted from the Meteonorm 5.1 software [32]. The simulation period was from December 21st to March 21st and the simulation time step was 1 h.

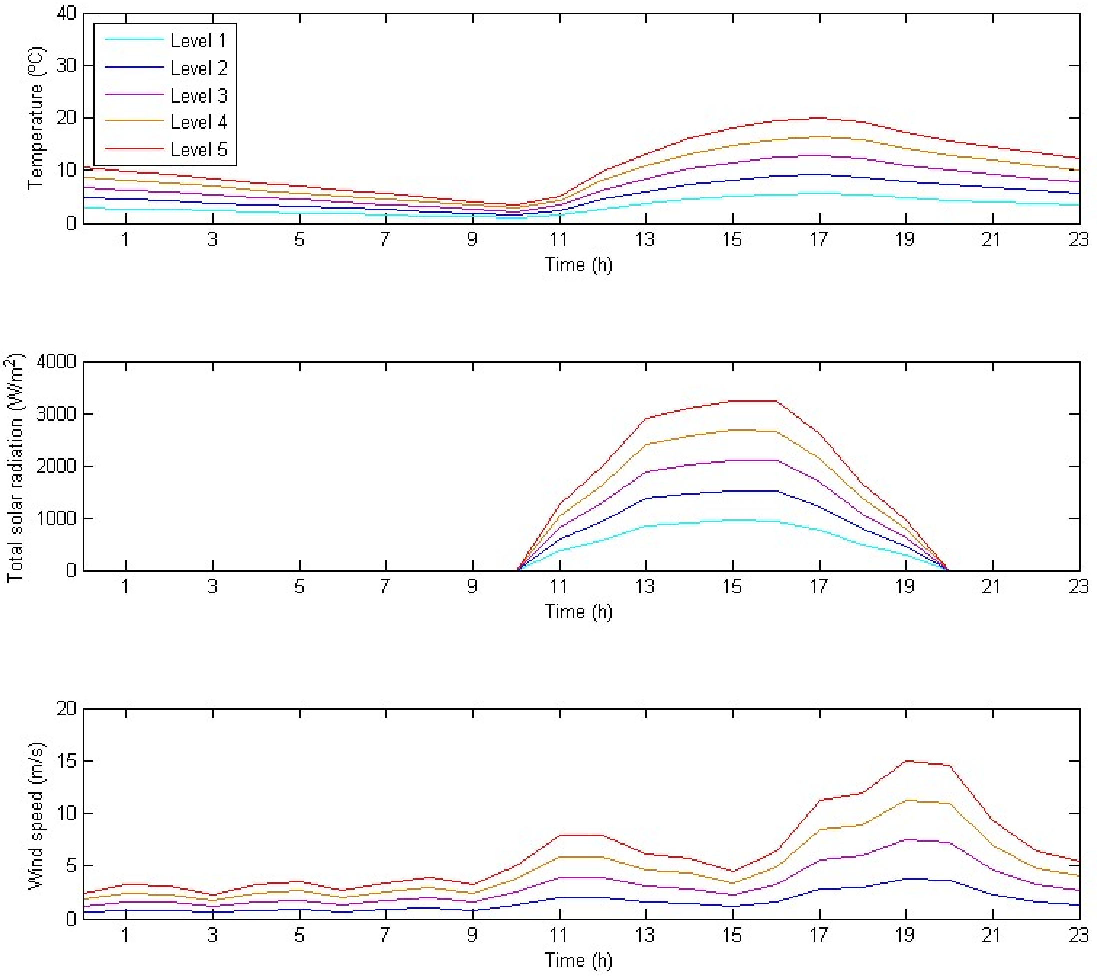

Figure 4. Hourly levels of temperature, total solar radiation on the façade and wind speed used for the sensitivity analysis

Figure 5. Map of climates zones in Spain

Table 6. Climatic zones in Spain according to climate severity

SC (Summer)					
	A4	B4	C4		E1
	A3	B3	C3	D3	
			C2	D2	
			C1	D1	
		SC (Winter)			

Table 7. Locations selected for each climatic zone (e=elevation)

Climatic Zone	Town
A3	Cádiz 36˚53'N 4˚46'O e=120 m
A4	Almeria 36 ˚50'N 2 ˚27'O e=27 m

Climatic Zone	Town
B3	Valencia 39 ˚28'N 0 ˚22'O e=15 m
B4	Córdoba 37 ˚53' N 4 ˚46' O e=120 m

Climatic Zone	Town
C1	Oviedo 43 ˚21' N 5 ˚51' O e=250
C2	Orense 42 ˚20'N 7 ˚51' O e=145 m
C3	Granada 37 ˚10'N 3 ˚36'O e=738 m
C4	Badajoz 38 ˚53' N 6 ˚58' O e=184 m

Climatic Zone	Town
D1	Vitoria 42 ˚51N 2 ˚40' O e=525 m
D2	Salamanca 40 ˚57'N 5 ˚39'O e=798 m
D3	Zaragoza 41 ˚39'N 0 ˚53'O e=200 m

Climatic Zone	Town
E1	Burgos 42 ˚21'N 3 ˚41'O e=856 m

3. Results

In figure 6 the heating demand is shown on a daily basis (only working days) for the climatic zone B4 and for the same office room with and without OVF during the winter. It can be seen that the heating demand was lower using an OVF in all the working days. However the differences of heating demand were quite dispersed. On six days there wasn't any energy demand at all whereas the demand without OVF was positive. There were also days in which the energy demand was similar in both cases. The average energy demand in the case with OVF was 3.53 kWh whereas in the case without OVF was 6.17 kWh. Thus, installing an OVF system implied an energy saving of 43 % relative to the case without OVF.

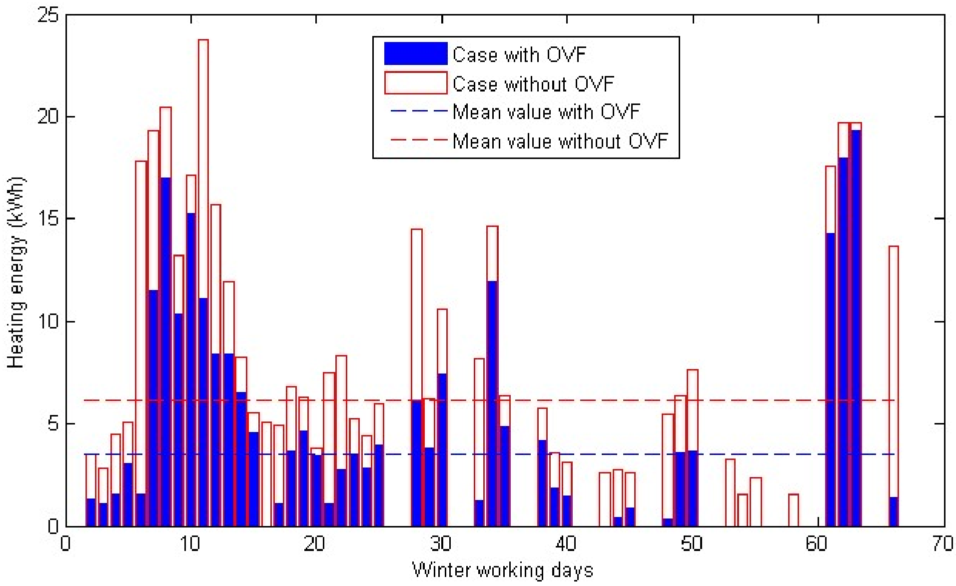

Figure 6. Comparison of heating energy demand between the buildings with and without OVF during working days in the winter season in location B4.

The variability in energy saving was due to the different weather condition each day. The most influential weather variables on the façade performance according to the numerical model were solar radiation on the façade, ambient temperature and wind speed and direction. However the influence of each variable in the energy saving cannot be explained in a simple way. Therefore a sensitivity analysis over the main weather variables was carried out. This way the most convenient climates to install an OVF and the more favourable type of days for a high heating energy saving can be found.

The result of the sensitivity analysis can be seen in figures 7-12 and in the results of the ANOVA analysis, tables 8 and 9. The effect of wind direction was not considered since in the model its effect on the external convection heat transfer coefficient only depended on whether the direction was windward or leeward. Figures 7, 9 and 11 represent the single effect of temperature, radiation and wind speed on daily heating energy saving for the 125 cases. Figures 8, 10 and 12 show the single effect of temperature, radiation and wind speed on OVF efficiency. In the case of radiation, figure 7, the general trend of mean energy saving was to increase as radiation increased. That was expected as the main source of heating of the OVF is beam solar radiation. The ANOVA analysis confirms this conclusion. In table 8 the sum of squares of the radiation parameter was clearly higher than those of temperature and wind speed. Solar radiation was the least influencing parameter on the OVF efficiency, figure 8. This result can also be obtained from the ANOVA results, table 9, and agrees with the results in other studies [20, 33].

It was also expected that the energy saving decreased when wind speed increased, as the higher wind speed implied greater convective heat transfer coefficients in equations 2 and 3 and thus more heat loss to the outside air and lower OVF efficiency, figures 11 and 12. The approaching wind effect has been studied widely in literature for UTC's. In this case the effect of wind speed on OVF efficiency can be compared with the effect of wind speed on UTC heat transfer effectiveness, as the UTC efficiency is also affected by the increasing air flow rates through the holes. The same trend can be found for both variables in [34].

A maximum value of mean energy saving was found for temperature in figure 9. In order to draw a conclusion from this evidence it was necessary to take into account the combined effect of temperature and solar radiation, since in the ANOVA analysis, table 8, the most influential combination was found to be that of these variables. In figure 13, it can be observed that at high radiation level, the energy saving decreased strongly, whereas at lower radiation levels the slope was lower. It can also be observed that the maximum energy saving found in figure 9 depended on the wind speed. As the wind speed level increased, the temperature for the maximum energy saving shifted to higher values. Since temperatures are not normally so high in the winter, with high wind speeds, above level three, this optimum temperature cannot be reached and the energy saving eventually increase only with radiation and temperature. The opposite trend was found for OVF efficiency, figure 10, although its influence was weak, table 9.A similar result can be encountered in [34].

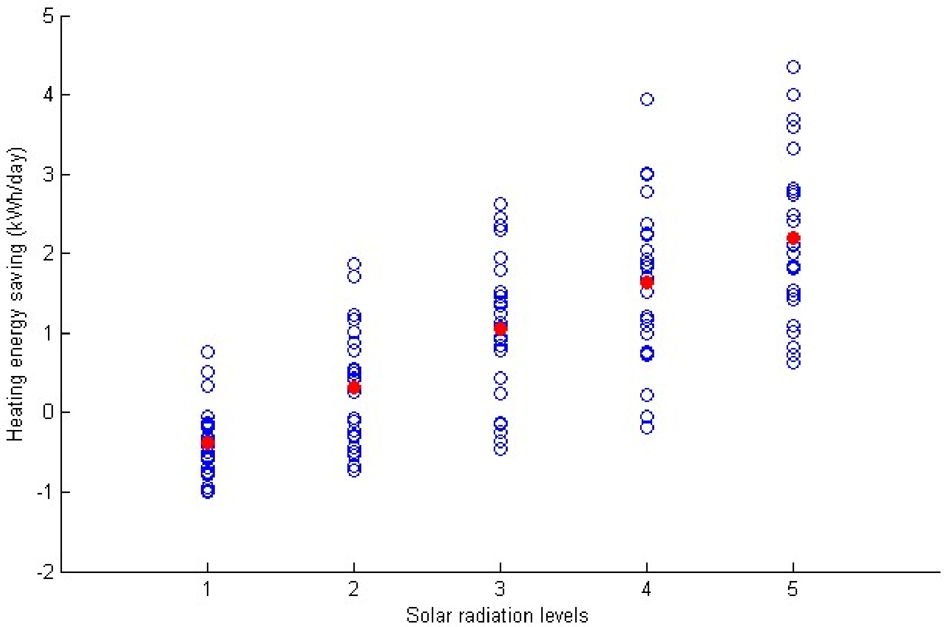

Figure 7. Scatter diagram of heating demand depending on the total solar radiation levels selected. The mean values are in red.

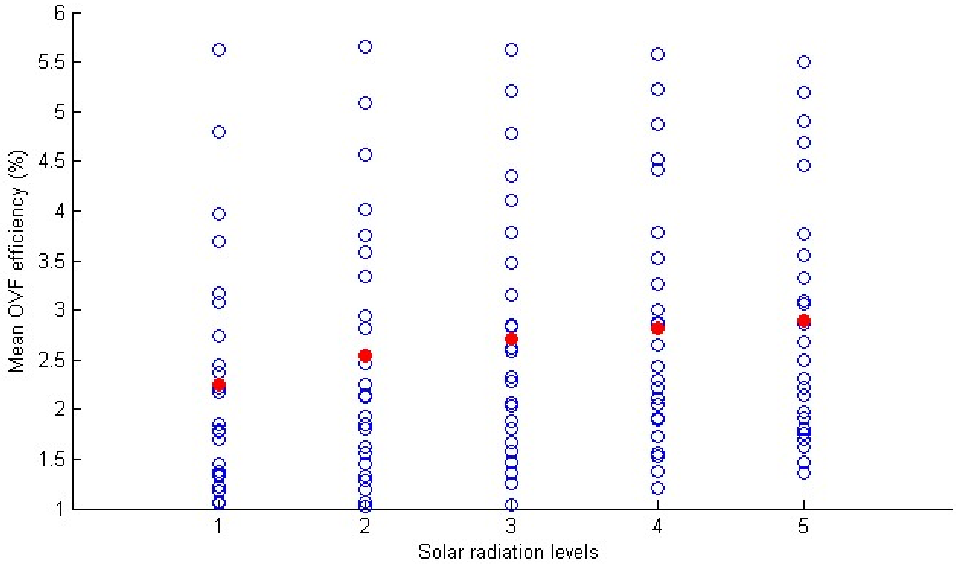

Figure 8. Scatter diagram of OVF efficiency depending on the total solar radiation levels selected. The mean values are in red.

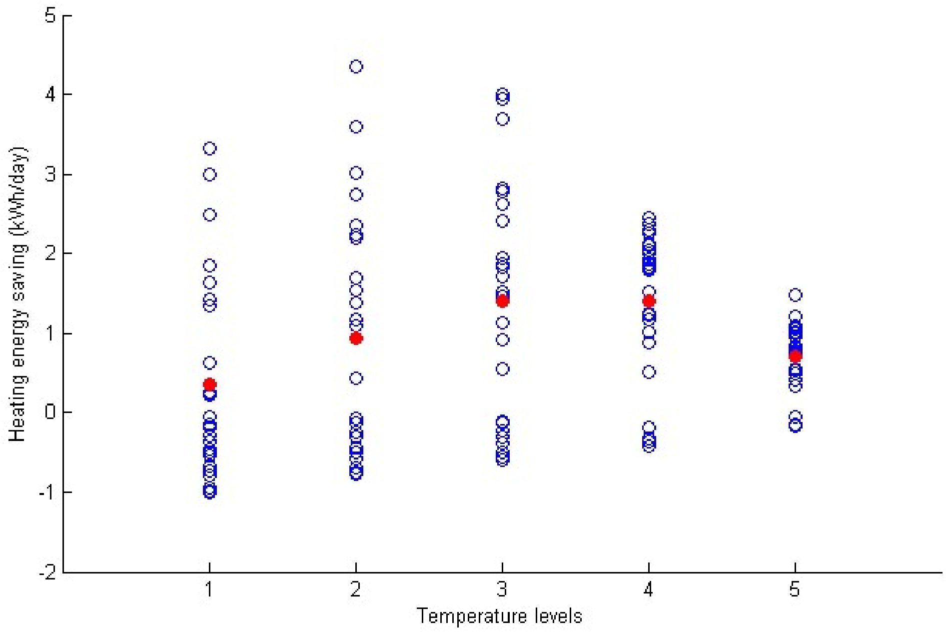

Figure 9. Scatter diagram of heating energy saving depending on the ambient temperature levels selected. The mean values are in red.

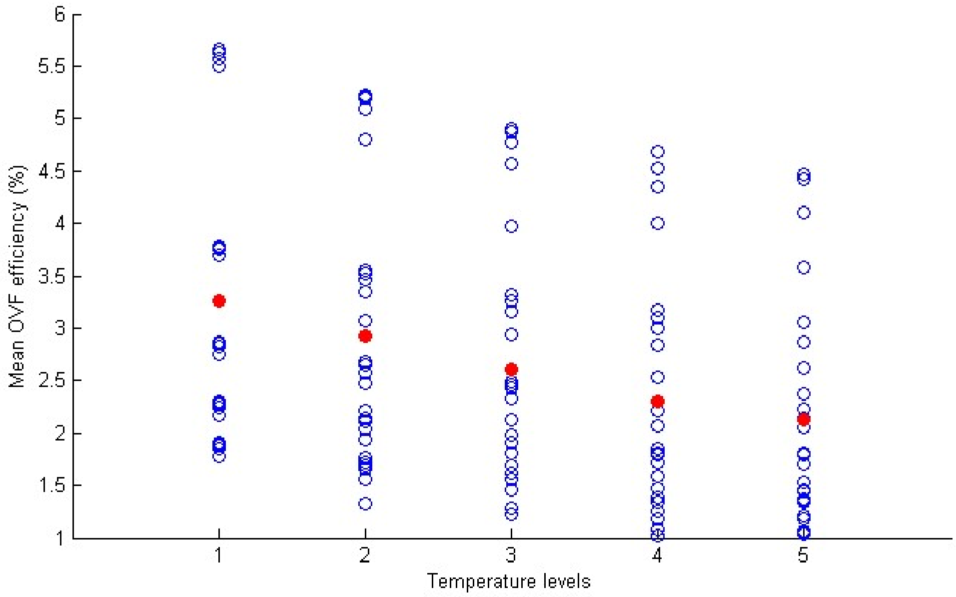

Figure 10. Scatter diagram of OVF efficiency depending on the ambient temperature levels selected. The mean values are in red.

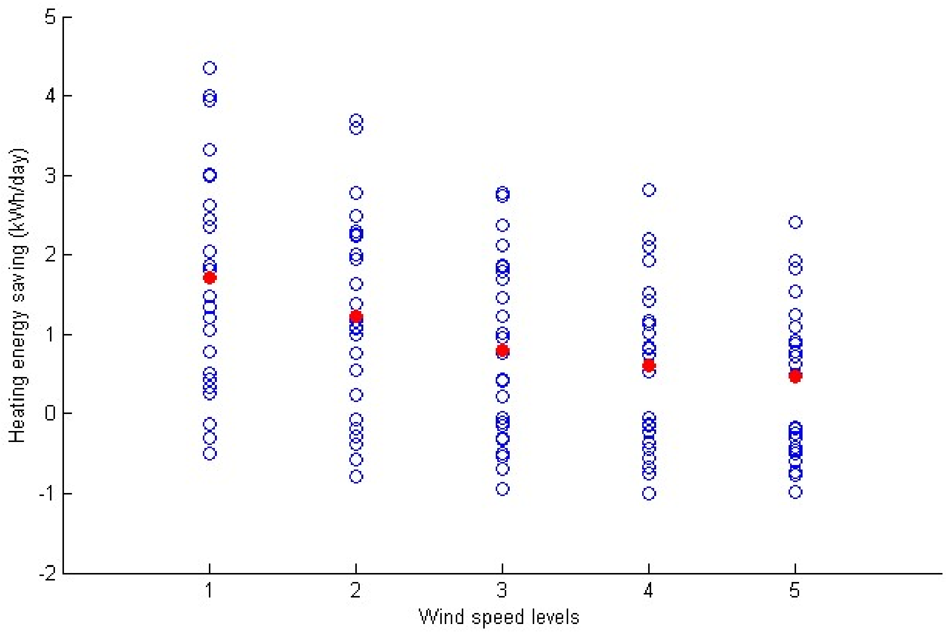

Figure 11. Scatter diagram of heating demand depending on the wind speed levels selected. The mean values are in red.

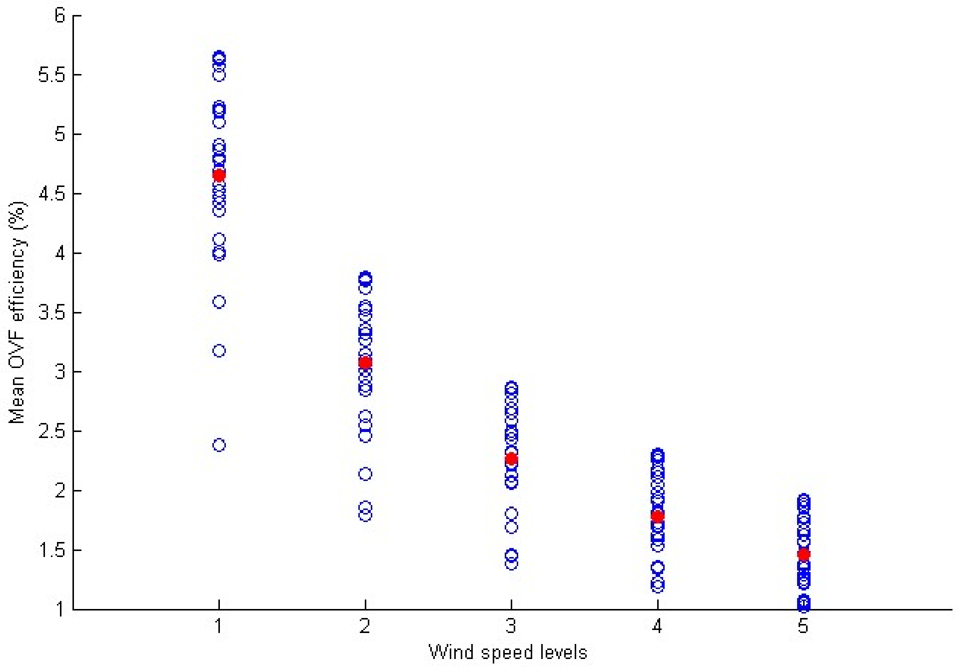

Figure 12. Scatter diagram of OVF efficiency depending on the ambient temperature levels selected. The mean values are in red.

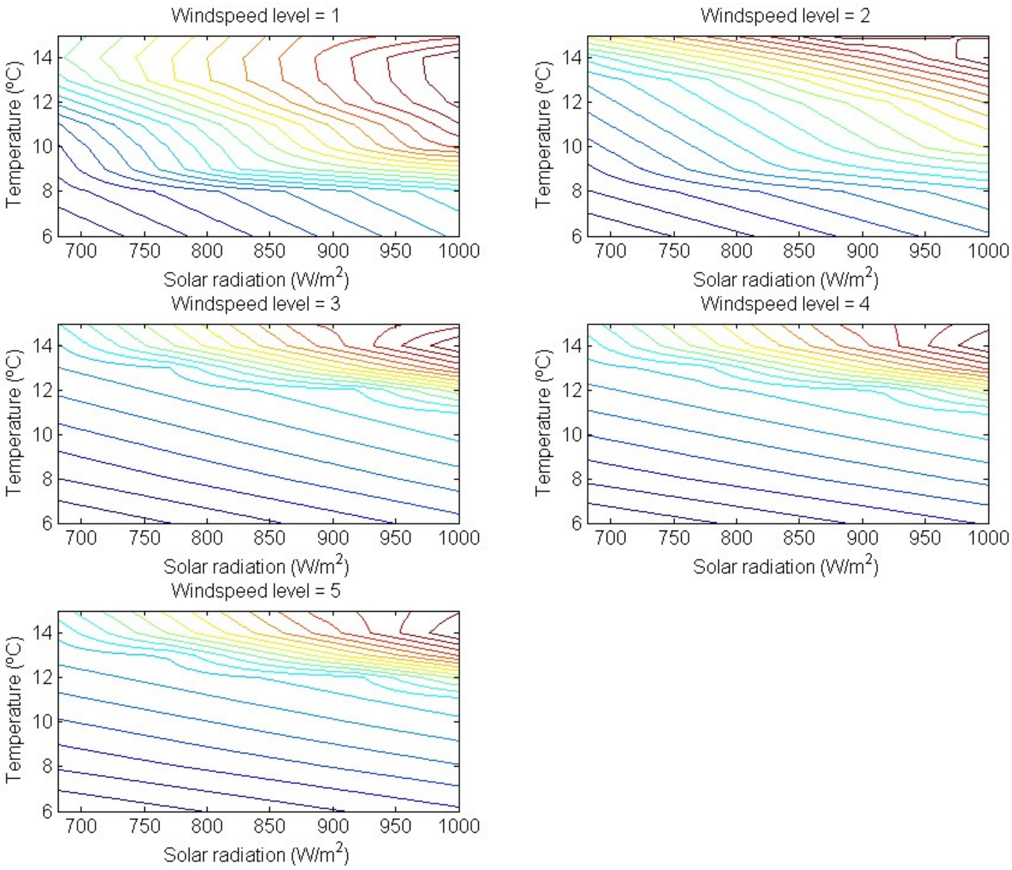

Figure 13. Contour plots of energy saving depending on ambient temperature and solar radiation for each wind speed level.

Table 8. Energy saving ANOVA results

SOURCE	SUM SQ.	D.F.	MEAN SQ.	F	PROB>F
X1 (TEMPERATURE)	20.761	4	5.1903	47.24	0
X2 (RADIATION)	105.173	4	26.2933	239.31	0
X3 (WIND SPEED)	25.889	4	6.4724	58.91	0
X1*X2	23.722	16	1.4826	13.49	0
X1*X3	5.945	16	0.3715	3.38	0.0003
X2*X3	3.112	16	0.1945	1.77	0.0557
ERROR	7.032	64	0.1099		
TOTAL	191.635	124			

Table 9. OVF efficiency ANOVA results

SOURCE	SUM SQ.	D.F.	MEAN SQ.	F	PROB>F
X1 (TEMPERATURE)	20.875	4	5.2187	224.16	0
X2 (RADIATION)	6.493	4	1.6233	69.73	0
X3 (WIND SPEED)	162.626	4	40.6564	1746.37	0
X1*X2	1.938	16	0.1211	5.2	0
X1*X3	2.393	16	0.1495	6.42	0
X2*X3	0.998	16	0.0624	2.68	0.0027
ERROR	1.49	64	0.0233		
TOTAL	196.812	124			

Therefore the performance of an OVF will be better in dry climates where sunny days prevail and the average wind speed is low. The advantage of using an OVF will be greater in climates with mild temperatures in the winter.

Figure 14 shows the winter energy saving evaluated for 12 locations corresponding to the 12 climatic zones in table 6. The locations were sorted by increasing winter severity and decreasing summer severity. In order to study the correspondence of these results with the previous sensibility analysis, the cumulative distribution function of solar radiation on the façade, ambient temperatures and wind speed were represented for each location in figures 15, 16 and 17.

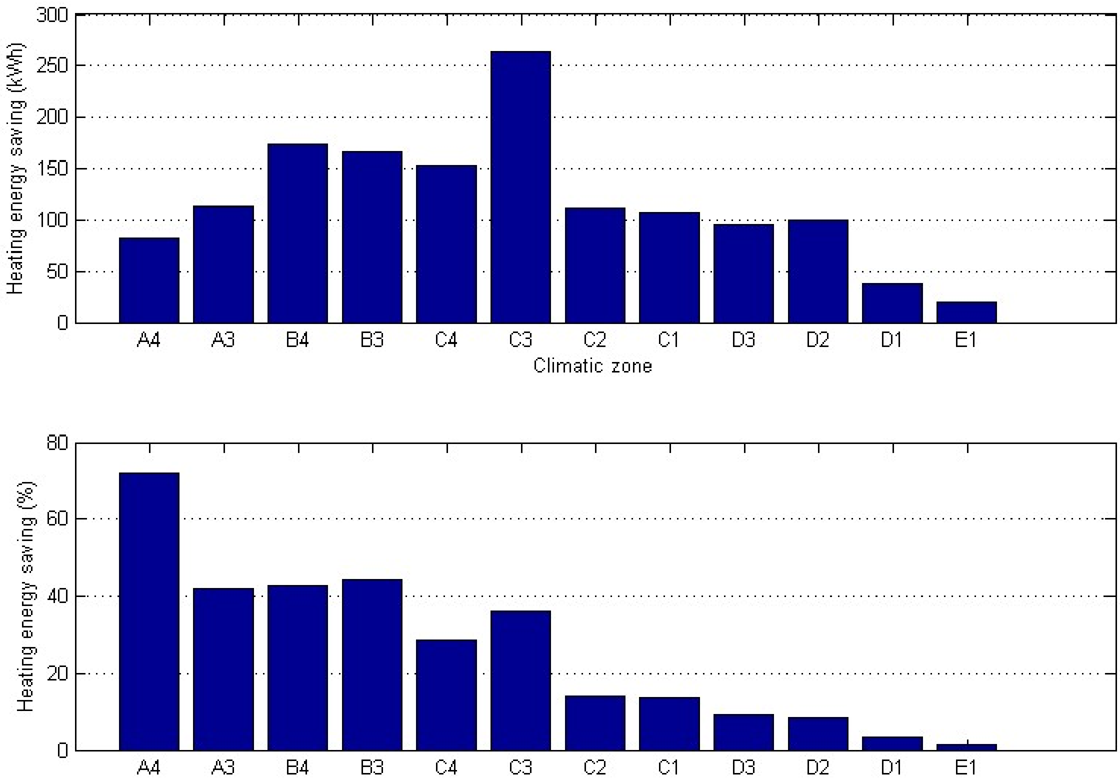

Figure 14. Winter season sensible heating energy saving using an OVF related to the same building without OVF in each location. Absolute and percentage values.

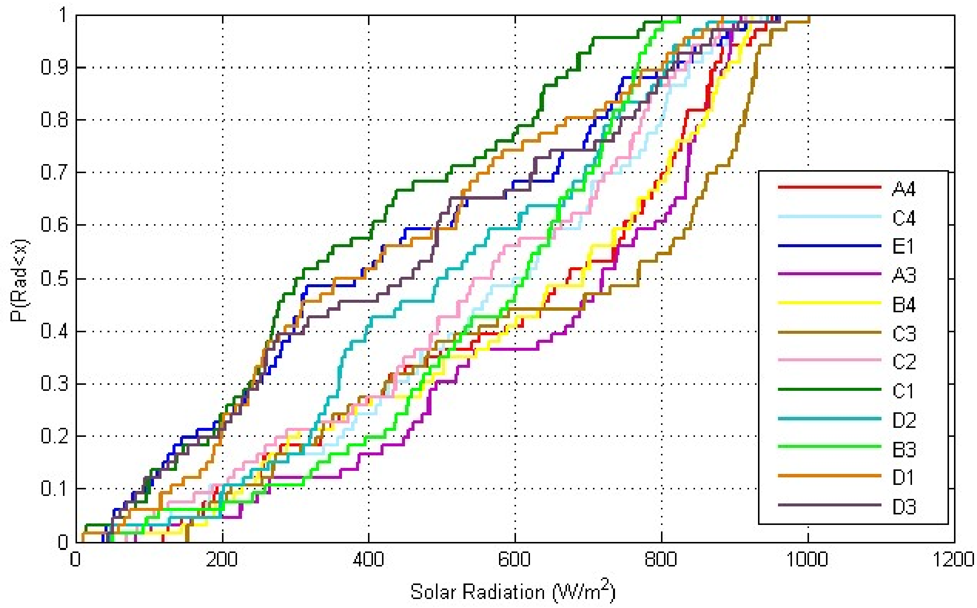

Figure 15. Solar radiation cumulative distribution functions for each location.

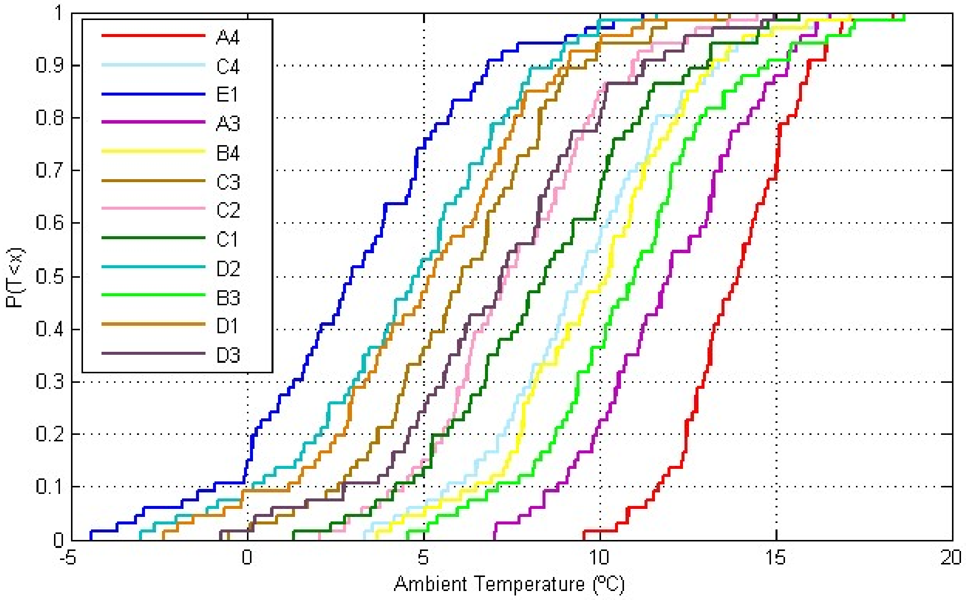

Figure 16. Ambient Temperature cumulative distribution functions for each location.

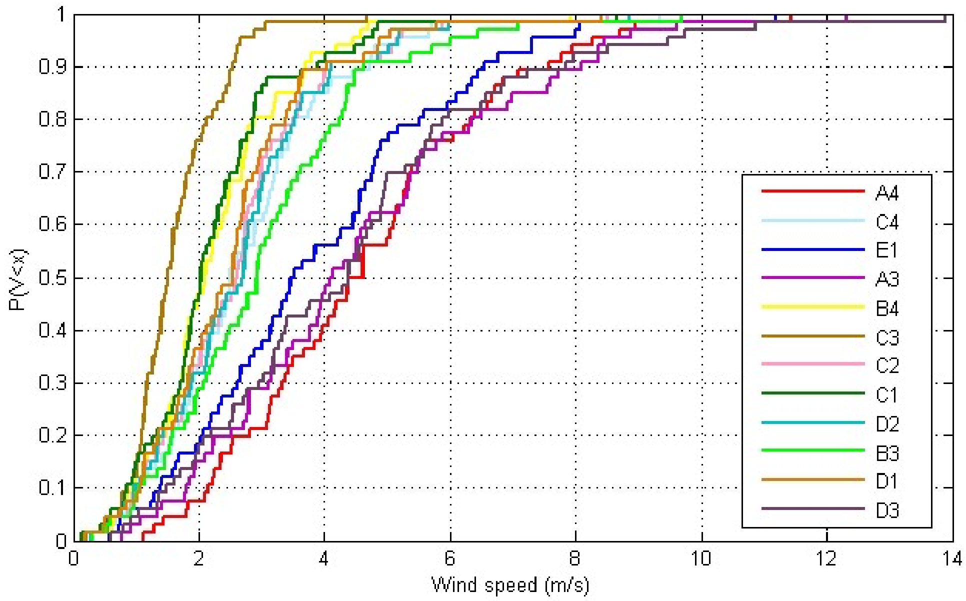

Figure 17. Wind speed cumulative distribution functions for each location.

Regarding radiation it can be observed that the greater energy saving in absolute terms were the locations with medium winter severity. Most of the locations with high energy saving corresponded with locations with a high level of radiation. The case of location C1 is remarkable, because despite having the lowest radiation distribution function its temperature level is higher and its wind speed the lowest of all, so it had a good level of energy saving, comparable with locations with higher solar radiation levels. It's also remarkable the case of location A4. This location had the second highest solar radiation level and the highest temperature distribution, however its energy saving resulted lower because of the high wind speed levels.

Regarding temperature, in general the locations with higher temperatures corresponded with the ones with higher energy saving. The exceptions were the case of A4, described above and the case of location C3, which had a low temperature but a high radiation and low wind speed levels. Looking at the wind speed levels, again, the lower levels of wind speed corresponded with the higher energy saving locations, with the exception of location A3 aforementioned and locations D1 and D2, which had low levels of radiation and temperature.

The same results were represented in figure 14 in terms of percentage of energy saving relative to the energy consumption without OVF. It can be observed that unlike the absolute values, percentages were almost inversely proportional to winter severity. The reason for this is that although energy saving could be low for low winter severity locations, the heating energy needed is also low, so most of the heating demand can be accomplished only by using the OVF.

The opposite was also true for the coldest climates. The clear exception to this rule of thumb was location C3. In this case, the energy saving was high, due mainly to the high solar radiation levels, and the percentage of energy saving resulted very high despite being a location with low temperatures.

These results agreed with the sensitivity analysis. Thus, it's possible to estimate the benefits of using an OVF in a certain location by collecting information about the weather data variables of that location along the winter.

4. Conclusions

In this study the combined effects of weather variables on the performance of an OVF was studied in an office building during the winter season. With the results obtained a study on the better locations in Spain to install an OVF was carried out. The main conclusions drawn from this paper were the following:

1. The most influential weather variable on the heat demand was the solar radiation on the façade. Temperature and wind speed were found to be also influential. Energy saving increased as solar radiation and ambient air temperature increased, whereas the energy saving had a maximum value for constant radiation and wind speed values at a certain temperature. The most influential combined effect was that of solar radiation and ambient temperature.
2. Energy saving in the winter were found to be positive for all the locations simulated in Spain.
3. The best locations to install an OVF in Spain were in the southern regions and the coastal areas, climatic zones A3, B3, B4, C3 and C4. They corresponded with those with the highest levels of solar radiation. Locations with lower solar radiation levels had high energy saving values when their temperatures levels were high and/or the average wind speed levels were low.
4. In general, the best locations to install an OVF were those with medium winter severity climate in absolute terms and low winter severity climate in relative terms.

Further study should be done to evaluate the impact of using an OVF in the summer period. It must also be studied the most convenient ventilation strategy in this case.

5. References:

[1] Quesada, G., et al., *A comprehensive review of solar façades. Transparent and translucent solar façades.* Renewable and Sustainable Energy Reviews, 2012. **16**(5): p. 2643-2651.
[2] Gratia, E. and A. De Herde, *Are energy consumptions decreased with the addition of a double-skin?* Energy and Buildings, 2007. **39**(5): p. 605-619.
[3] Holmes, M.J., *Optimisation of the thermal performance of mechanically and naturally ventilated glazed façades.* Renewable Energy, 1994. **5**(5–8): p. 1091-1098.
[4] Quesada, G., et al., *A comprehensive review of solar façades. Opaque solar façades.* Renewable and Sustainable Energy Reviews, 2012. **16**(5): p. 2820-2832.
[5] Cianfrini, C., et al., *Energy performance of a lightweight opaque ventilated façade integrated with the HVAC system using saturated exhaust indoor air.* Energy and Buildings, 2012. **50**(0): p. 26-34.

[6] Matuska, T. and B. Sourek, *Façade solar collectors.* Solar Energy, 2006. **80**(11): p. 1443-1452.
[7] Zogou, O. and H. Stapountzis, *Experimental validation of an improved concept of building integrated photovoltaic panels.* Renewable Energy, 2011. **36**(12): p. 3488-3498.
[8] Giancola, E., et al., *Experimental assessment and modelling of the performance of an open joint ventilated façade during actual operating conditions in Mediterranean climate.* Energy and Buildings, 2012. **54**(0): p. 363-375.
[9] Marinosci, C., G. Semprini, and G.L. Morini, *Experimental analysis of the summer thermal performances of a naturally ventilated rainscreen façade building.* Energy and Buildings, 2014. **72**: p. 280-287.
[10] Sanjuan, C., et al., *Energy performance of an open-joint ventilated façade compared with a conventional sealed cavity façade.* Solar Energy, 2011. **85**(9): p. 1851-1863.
[11] Seferis, P., et al., *Investigation of the performance of a ventilated wall.* Energy and Buildings, 2011. **43**(9): p. 2167-2178.
[12] Stazi, F., et al., *Experimental evaluation of ventilated walls with an external clay cladding.* Renewable Energy, 2011. **36**(12): p. 3373-3385.
[13] Marinosci, C., et al., *Empirical validation and modelling of a naturally ventilated rainscreen façade building.* Energy and Buildings, 2011. **43**(4): p. 853-863.
[14] Stazi, F., A. Vegliò, and C. Di Perna, *Experimental assessment of a zinc-titanium ventilated façade in a Mediterranean climate.* Energy and Buildings, 2014. **69**(0): p. 525-534.
[15] *US DOE EEERE at NREL.Research Support Facility. Leadership in Building Performance.* 2011; Available from: http://www.nrel.gov/sustainable_nrel/pdfs/51742.pdf.
[16] Shukla, A., et al., *A state of art review on the performance of transpired solar collector.* Renewable and Sustainable Energy Reviews, 2012. **16**(6): p. 3975-3985.
[17] Hollick, J.C., *Unglazed solar wall air heaters.* Renewable Energy, 1994. **5**(1–4): p. 415-421.
[18] FEMP, *Transpired Collectors (Solar Preheaters for Outdoor Ventilation Air).* Federal Technology Alert, 1998.
[19] Kutscher, C.F., C.B. Christensen, and G.M. Barker, *Unglazed Transpired Solar Collectors: Heat Loss Theory.* Journal of Solar Energy Engineering, 1993. **115**(3): p. 182-188.
[20] Chan, H.-Y., et al., *Thermal Analysis of Flat and Transpired Solar Façades.* Energy Procedia, 2014. **48**(0): p. 1345-1354.
[21] Saelens, D., S. Roels, and H. Hens, *Strategies to improve the energy performance of multiple-skin façades.* Building and Environment, 2008. **43**(4): p. 638-650.
[22] Kim, Y.-M., et al., *Contribution of natural ventilation in a double skin envelope to heating load reduction in winter.* Building and Environment, 2009. **44**(11): p. 2236-2244.
[23] Zamora, B. and A.S. Kaiser, *Numerical study on mixed buoyancy-wind driving induced flow in a solar chimney for building ventilation.* Renewable Energy, 2010. **35**(9): p. 2080-2088.
[24] López, F.P., et al., *Experimental analysis and model validation of an opaque ventilated façade.* Building and Environment, 2012. **56**(0): p. 265-275.
[25] UoW-M, S.E.L., *TRNSYS 16 Reference Manual*. 2004, GmbH TE, CSTB, TESS.
[26] AENOR, *ISO-EN-7730-2005 Ergonomics of the thermal environment –Analytical determination and interpretation of thermal comfort using calculation of the PMV and PPD indices and local thermal comfort effects.* 2006.
[27] AENOR, *RITE (Regulation of Thermal Installations in Buildings) IT 1.1.4.2.2*. 2011.
[28] Grosso, M., *Wind pressure distribution around buildings: a parametrical model.* Energy and Buildings, 1992. **18**(2): p. 101-131.
[29] Palyvos, J.A., *A survey of wind convection coefficient correlations for building envelope energy systems' modeling.* Applied Thermal Engineering, 2008. **28**(8–9): p. 801-808.
[30] Montgomery, D.C., *Desing and Analysis of Experiments*. 5º ed. 2001: John Wiley & Sons, INC.

[31] *CTE (Código Técnico de la Edificación)*. 2006, Ministerio de la Vivienda. Gobierno de España.
[32] Remund J., K.S., Schilter C., Muller S., *METEONORM Version 6.0 Handbook*. 2010.
[33] Badache, M., et al., *Experimental and Two-dimensional Numerical Simulation of an Unglazed Transpired Solar Air Collector.* Energy Procedia, 2012. **30**(0): p. 19-28.
[34] Leon, M.A. and S. Kumar, *Mathematical modeling and thermal performance analysis of unglazed transpired solar collectors.* Solar Energy, 2007. **81**(1): p. 62-75.